AIAA 81-0391R

Sources and Detection of Atmospheric Wind Shear

Alfred J. Bedard Jr.*
NOAA/ERL/Wave Propagation Laboratory, Boulder, Colo.

This paper outlines a range of phenomena producing significant atmospheric wind shears, providing more details on the shears related to thunderstorm gust fronts. A case study from a wintertime Colorado front-range experiment during 1980 documents strong wind gradients that can occur in the lees of mountains. Strengths and weaknesses of some detection methods are discussed, and evaluations of both remote-sensor and in situ sensor approaches for detecting atmospheric wind shear are emphasized.

Introduction

AIRCRAFT can encounter dangerous wind shear on a variety of scales from a great number of sources both natural and man-made. Table 1 indicates the broad range and scale sizes of wind shear phenomena contributing to the problem. The forms of atmospheric wind shear occurring both singly and in combination represent a significant hazard to aircraft operations.[1] When various wind shear mechanisms occur in combination, the detection problem can become more difficult. Examples of these combined hazards can involve a ground-based inversion with an evolving flowfield just above the top. Such conditions can occur in the lee of obstacles as well as when thunderstorm flows interact with stable layers. The motions of wake vortices are more complex in a turbulent, layered atmosphere. It is a challenge to develop a single, integrated system for sensing these hazards. Although methods exist for providing operational warnings for some types of wind shear (e.g., thunderstorm outflows)[2,3], practical detection methods have yet to be developed for other forms (e.g., concentrated thunderstorm downflows[4]).

Fujita[5] documented the properties of thunderstorm downflow regions in some detail. This paper concentrates on properties of thunderstorm outflows involved in a number of recent air-carrier incidents. In addition, a detailed case study involving obstacle shear flow/stable layer interactions emphasizes how different detection methods (e.g., well-situated surface sensors or vertically pointing remote sensors) can be effective for different types of hazards.

There are several ways of looking at the characteristic scales of phenomena. One important dimension involves the horizontal or vertical widths of transition regions (e.g., the leading edges of gust fronts). Another important dimension is the scale sizes over which the phenomenon occurs (e.g., the circumference of the outflow field). While the smaller scale of the transition zone can be a measure of the potential for danger to an aircraft, the larger scale size of the phenomena is a measure of the probability of encountering the system. An additional scale size is that related to the waves and turbulence that can often accompany a region of strong shear. These smaller-scale fluctuations compound the problem of making an appropriate control response to a mean shear condition or, if intense enough, can represent a control problem independent of the mean shear.

In this regard, Houbolt[6] points out frequency ranges of importance for various aspects of aircraft control (e.g., pilot influence, aircraft phugoid, navigation). In terms of wavelength, Vinnichenko et al.[20] indicate that perturbations with lengths in the range from 10 m to 7 km can be important for subsonic aircraft whereas wavelengths up to 20 km can affect supersonic aircraft. Where data are available, Table 1 also includes information on the smaller scales accompanying wind shear mechanisms. MacCready[7] finds that the spectrum law based upon inertial subrange assumptions approximates observed data up to wavelengths of several hundred meters. Panofsky and Press[8] also provide an excellent review of atmospheric turbulence measurements applied to aeronautics.

Presented as Paper 81-0391 at the AIAA 19th Aerospace Sciences Meeting, St. Louis, Mo., Jan. 12-15, 1981; submitted March 10, 1981; revision received Nov. 6, 1981. This paper is declared a work of the U. S. Government and therefore is in the public domain.

*Physicist.

Combinations of Hazards

The fact that various hazardous shears can occur together can complicate a situation already difficult to detect and analyze; for example, an inversion wind shear situation can be eliminated by a thunderstorm outflow[2] whereas an inversion can prevent a potentially hazardous gust front from being sensed at ground level.[22]

Thunderstorm Outflow/Downflow Shears

Although data from the Thunderstorm Project[11] still remain an important resource for documenting the properties of severe storms, more recent studies have expanded the data base available for thunderstorm downflow/outflow systems. It may seem arbitrary to distinguish thunderstorm downflow and outflow fields as two forms of shear since the downflow/outflow fields are really one system. In practice, however, this distinction is important because one hazardous region (the leading edge of the outflow) can occur at large distances (10 to 20 km) from another hazardous region (the downflow region). Moreover, detection methods applicable to the leading edge of the outflow region (relatively sparse arrays of surface sensors or single Doppler radars) may not apply to a concentrated (<1 km diameter) downflow region. Hence, these two aspects of thunderstorm shear can be treated as separate detection problems.

Thunderstorm Outflows

The properties and detection of thunderstorm outflows were the subject of several recent investigations.[2,3,9,23] These and related studies produced data sets valuable not only for describing the flowfields of outflow currents for simulating aircraft response[24,25] or remote-sensor operation[26] but also for evaluating in-situ surface sensor arrays as detection systems. The largest temperature drops and pressure jumps usually accompany the strongest outflow systems and greater degree of hazard.[2] Several concepts for use of surface arrays evolved from these studies, including anemometer arrays[3] and a combined pressure sensor/anemometer system.[2] Table 2 summarizes thunderstorm properties determined from several sources. Some differences in properties previously reported in various studies may reflect regional differences in thunderstorm characteristics as well as differences in measurement techniques. Unless indicated, the properties listed in Table 2 derive from the work of Bedard et al.[2] There is a great need for more detailed measurements of thunderstorm downflows describing the evolution of the flow from near cloud base to the surface.

Table 1 Sources of wind shear

Source	Scales of phenomena	Scales of transition regions	Scales of waves or turbulence
Thunderstorm outflows	Outflow diam 2-100 km (Ref. 2) Outflow height 400-600 m (Ref. 2)	Horizontal width 2-5 km (Refs. 2,3,9,10)	—
Thunderstorm downflows	Downflow diam 0.3-7 km (Ref. 11) 0.8-8 km from widths of damage paths (Ref. 5) Height of downflow region 3-5 km	Horizontal width estimate: over a horizontal region, on the scale of about 1/10 the downflow diameter Variation of vertical wind speed with height near the surface: estimate, over a vertical region above the surface, on the scale of the downflow diameter	8-270 m (Ref. 11)
Nocturnal jet above a surface-based inversion	Vertical scale 10s to 100s of m (this paper) Horizontal scales 10s of km by 100s of km (Ref. 12)	Vertical widths 10s to 100s of m (this paper)	Wave activity wavelengths 0.5-7 km (Ref. 13)
Cold-front systems	Horizontal scales 100s of km Vertical slopes of interface between cold and warm air from 1/50 to 1/100 or even steeper (Ref. 14)	—	—
Warm-front systems	Horizontal scales 100s of km Vertical slopes of interface between warm and cold air from 1/100 to 1/300 or even shallower (Ref. 14)	—	—
Downslope windstorm situations	Horizontal scales 10s of km by 100s of km (Ref. 15) Vertical scales surface to above 10 km	Kilometers to 10s of km (Refs. 15 and 16)	0.3-20 km (Ref. 15)
Obstacle/flow effects	Vertical dimensions several obstacle scale heights Horizontal dimensions to 10s of obstacle scale heights (Ref. 17)	—	—
Wake vortex systems	Horizontal scales 10s of m by 10s of km (Ref. 18)	Smaller than the wind span of the generating aircraft	Sinusoidal instabilities of the vortex axes on scales of 10s of meters (Ref. 19)
Gravity/shear waves at jet stream altitudes	Vertical height 1-15 km Horizontal scales 100s of km Vertical scales kilometers (Ref. 20)	Horizontal and vertical widths 10s of km (Ref. 20)	Wavelengths 4-20 km (Ref. 21)

Obstacle Shear Flow/Stable Layer Interactions

In the vicinity of mountain ranges, various types of atmospheric wind shears can occur in combination. Furthermore, as the volume and variety of air traffic increase near mountainous regions, types of obstacle shear flows will present more of a hazard. One case study from a 1980 front-range experiment provides an example of lee-side wind shear and illustrates how remote sensors [in this case a monostatic acoustic sounder and a FM/continuous-wave (CW) radar] and well-situated surface-measuring sites can provide warnings of hazardous conditions. This example indicates one type of obstacle shear flow, specifically, a complex obstacle shear flow interacting with stably stratified lee-side layers. Other complex flow patterns including the series of complex patterns described by Förchtgött[10] and other workers, exist in both steady and unsteady forms near obstacles.

Case Study Showing Erosion of a Stable Layer and Attendant Wind Shear and Turbulence

Figure 1 is an artist's view of processes in the lee of a mountain range detailed by measurements during Project AEOLUS 1980† which shows the erosion of a strong surface-based inversion by an upper-level flow. Key elements of the experiment involved the Portable Automated Mesonet (PAM) of the National Center for Atmospheric Research (NCAR)[27] as well as a variety of in situ sensors, remote sensors, aircraft probes, and rawinsonde launches. This experiment involved participants from a number of organizations, and we hope to document the complete experiment and the data sets at a later date. This case study of March 5-6, 1980 indicates only one of a broad range of phenomena influencing the front-range area. That the observations are typical of a meteorological scenario in the lee of a large mountain range can be seen from the statistical study of Hicks and Mathews,[28] who found that similar situations occur frequently in the Calgary area during winter.

Figure 2 shows the locations of some instruments in the Boulder, Colorado, area. In addition to the FM/CW radar,[29] a monostatic acoustic sounder operated near the Boulder Wind Network site TBL. Although many other measurements were made during Project AEOLUS, the elements noted above are most pertinent to this case study.

Several days before the March 5-6, 1980 event, a cold air mass from Canada left cool air and a snow cover along the front range. In the Boulder area a combination of the snow cover and clouds inhibited the breakup of a strong ground-based inversion. Under these conditions an approaching low-pressure area to the northwest caused an increased flow aloft on March 5-6, 1980.

Figure 3 presents the wind speed data for the PAM sites. Note that many totally calm sites show an abrupt wind speed increase commencing at about 2200 Mountain Standard Time (MST) on March 5. A similar presentation for temperature data (Fig. 4) shows temperature increases in excess of 12°C corresponding in time with the wind surges. The flow increase at PAM 13 (about 3000 ft above the Boulder Valley) occurred about 8 h before the flow increases at the lee-side sites. Also,

†Project AEOLUS 1980 was a front-range meteorological experiment held from January through March 1980. AEOLUS (the Greek god of the winds) stands for Atmospheric Experiment on Orographic flows, Leewaves, Upslope snow storms, Severe downslope wind storms.

Table 2 Observed properties of thunderstorm outflows, thunderstorm downflows, and frontal passages

Thunderstorm outflows and frontal passages	
Surface wind speed surges	0-15 m/s^{-1}
System propagation speed	5-38 m/s^{-1}
Surface wind vector changes	2-17 m/s^{-1}
Pressure-jump magnitudes	0.5-2 mbar most frequent
Surface-temperature changes	Range[a] $-12-+15°C$
Width of transition zone	Most frequent, 3-5 km; average, 2 km from Ref. 3 and 3 km from Ref. 10
Height of outflow	Most frequent, 400-600 m
Observed maximum propagation distances from downflow region	20-50 km
Thunderstorm downflows	
Downflow diameters	0.3-7 km (Ref. 11); 0.8-8 km (Ref. 5)
Downflow vertical velocities	Most frequent, ~10 m/s^{-1} (Ref. 11)
Maximum downflow pressure fields	Pressure nose of >5 mbar measured (equivalent to a downward speed of greater than 30 m/s^{-1})

[a]The observations of temperature increases can be explained by downward mixing of warm air resulting from the passage of a cold-air outflow above a cooler ground-based inversion.[22]

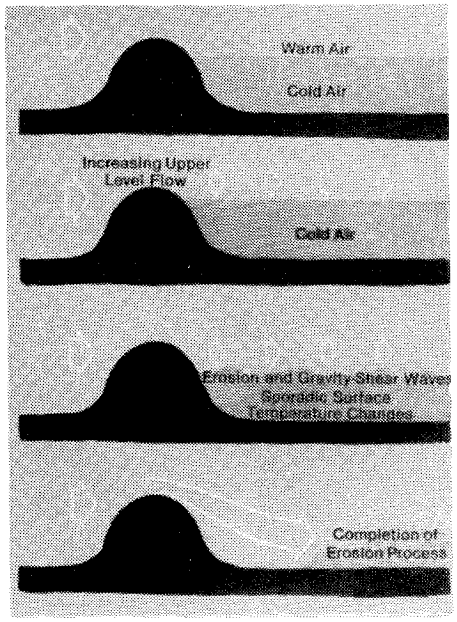

Fig. 1 Artist's view of the erosion of a ground-based, lee-side inversion by a warmer, upper-level flow.

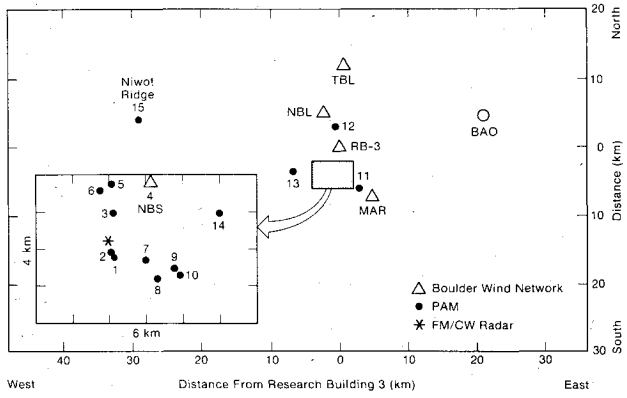

Fig. 2 Locations of instruments in the Boulder, Colo., area during Project AEOLUS 1980.

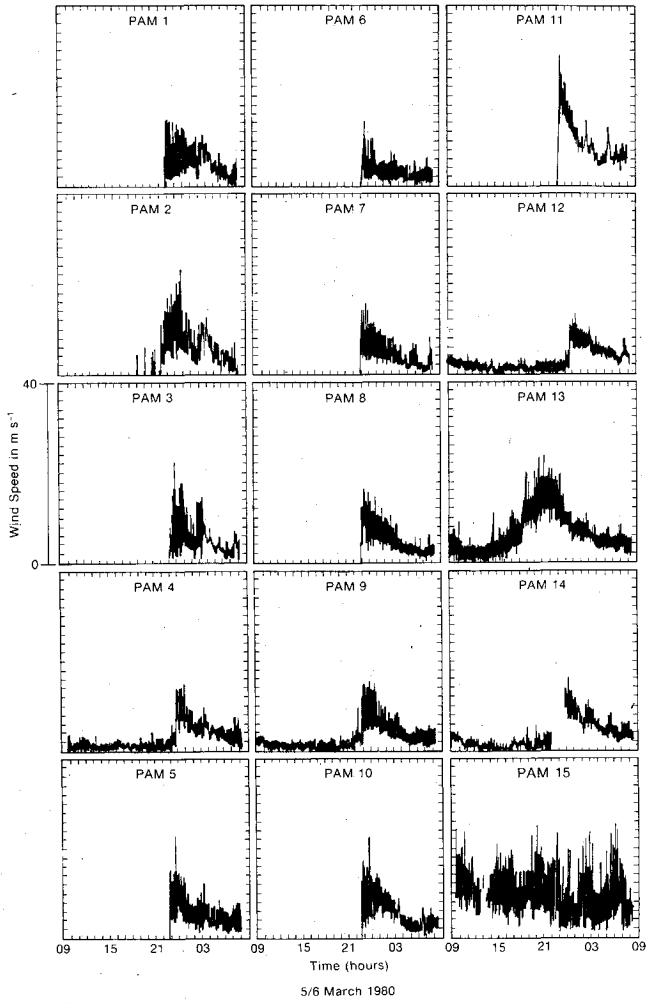

Fig. 3 Wind speed measurements from the PAM sites on March 5-6, 1980 (MST).

large sporadic temperature changes (Fig. 5) and wind speed surges preceded complete erosion of the inversion.

The mechanisms causing these abrupt changes are shown vividly by the monostatic acoustic sounder returns and associated TBL wind network measurements (taken about 200 yards west of the acoustic sounder). The vertical axes of the lower records of Figs. 6a and 6b are the wind speed in m s^{-1} (at the origin of the vectors). The vectors indicate the wind direction (an arrow pointing upward indicating a flow from the south). During the interval from 1500 to 2100 MST, when the wind speed increased above the Boulder Valley (PAM 13), the darkened region of the acoustic sounder record above 400 m indicates the existence of a shear layer. The intensity of the acoustic return is greater from regions of inhanced turbulent temperature fluctuations. Such variations occur from local increases in dynamic instability or local lapse rate conditions favoring increased thermal small-scale variability.[13] Thus, the light portions of the monostatic sounder record indicate regions of stability and the darker regions locate the unstable layers above the sounder. Between 2000 and 0100 MST this layer slowly approaches the surface attended by apparent wave activity and turbulence. One question addressed in a later section is whether the erosion rate could be estimated from the sounder record (and hence the impact time predicted) in spite of the effects of wave activity and turbulence. The intersection of this layer with the surface at about 0100 MST is accompanied by a sudden surge in surface wind speed and a change in wind direction. Nonlinear breakdown of the large-amplitude waves could explain the sudden surges in wind speed and temperature (Fig. 5) observed at some surface sites.

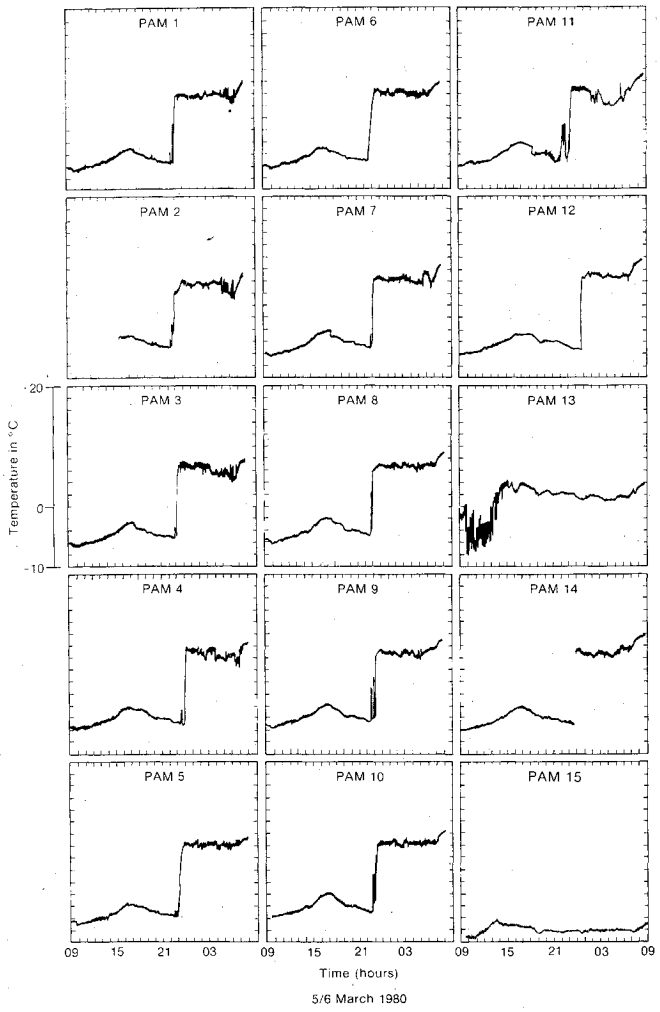

Fig. 4 Temperature measurements from the PAM sites on March 5-6, 1980 (MST).

Fortunately the FM/CW radar, controlled to point along the direction of the upper-level flow, also documented the inversion height and flow profile (Fig. 7). These data also indicate a strong shear occurring near mountaintop levels and slowly decreasing in altitude as a function of time. If the times at which the temperature stabilized at the higher value (Fig. 4) are plotted as a function of height above sea level, an approximately constant rate of erosion is inferred independent of measurement position in the Boulder area.

Bell and Thompson,[30] in numerical analyses and laboratory experiments, investigate the conditions under which ventilation of a valley filled with stable air is initiated. Using the Froude number as a criterion, they find that the onset of ventilation can be predicted.

To test this criterion for the onset of erosion for our case study, PAM site 13 is used to specify the upper-level flow magnitude and the initial height of the inversion. Based on an inversion height of 1 km and a temperature difference of 12°C, the Froude number for several PAM 13 wind speeds appears in Fig. 8. For these calculations the Froude number (F_r) was defined as

$$F_r = \frac{U}{[(\Delta T/T)gh]^{1/2}}$$

where U is the wind speed above the inversion, h the inversion height, g the local gravitational acceleration, ΔT the temperature difference, and T the mean temperature.

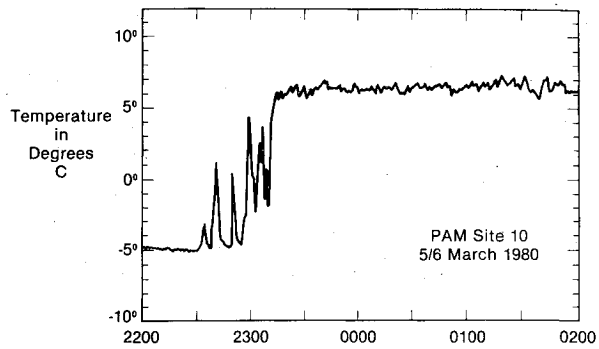

Fig. 5 Sporadic temperature changes for PAM site 10 associated with the inversion breakdown. Time is MST.

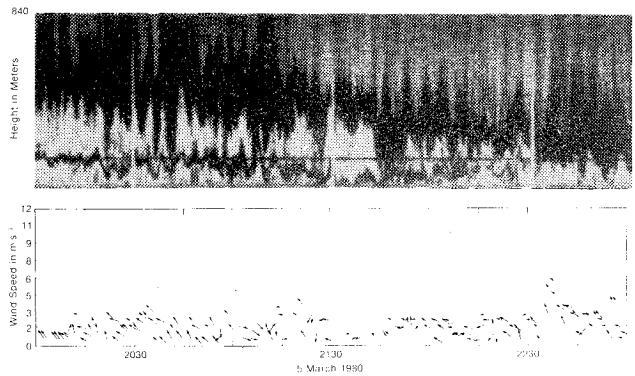

Fig. 6a Monostatic acoustic sounder record and wind speed/direction plot for site TBL from 2000 to 2300 MST.

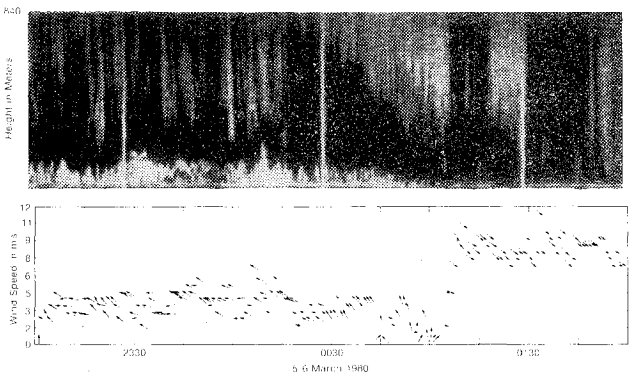

Fig. 6b Monostatic acoustic sounder record and wind speed/direction plot for site TBL from 2300 to 0200 MST.

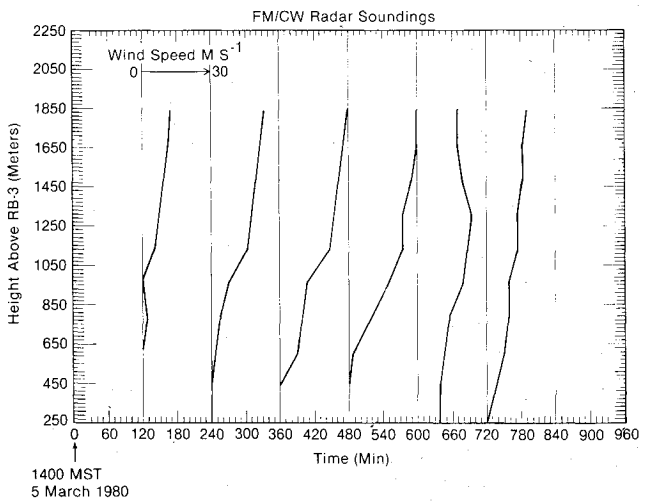

Fig. 7 FM/CW radar wind profiles at 2-h intervals.

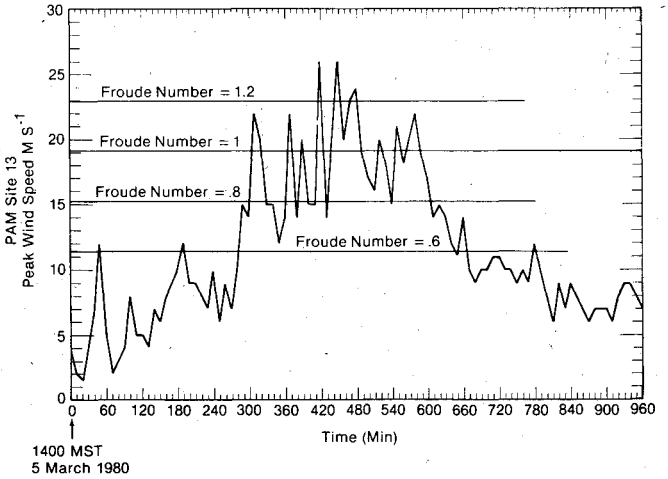

Fig. 8 PAM site 13 wind speed/Froude number comparison.

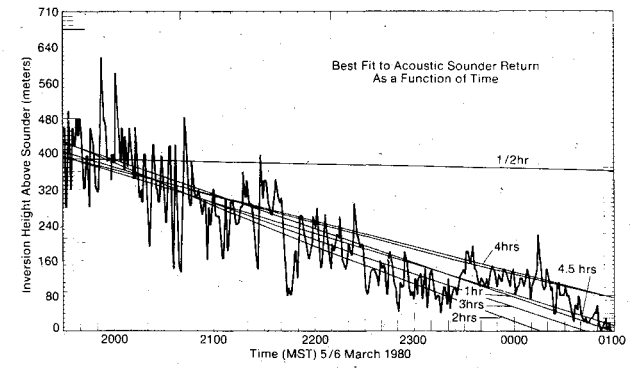

Fig. 9 Test of the feasibility of predicting erosion impact with surface from acoustic sounder returns complicated by wave activity and turbulence.

The erosion process started when F_r exceeded a value $F_r = 1$, indicating that the inertial forces started to exceed the negative buoyancy forces.

Practical Implications of This Case Study for Detection and Warning

Several results of this case study have implications for providing warning of this type of shear, especially when it occurs in combination with orographic features.

1) The FM/CW radar provided reliable clear air returns in this meteorological situation and can be applied to obtain wind profiles as well as to estimate inversion heights.

2) The value of a site at higher altitude overlooking a valley is indicated by Fig. 8. Temperature data from this site and a low-altitude site could indicate the inversion strength. Wind speed data can provide a basis for estimating the onset of an erosion process using a Froude number criterion.

3) In conjunction with a higher-altitude measurement site, a monostatic acoustic sounder can specify the height of an inversion as a function of time while the upper-level flow measurement serves as a basis for estimating the shear magnitude.

This section also addresses the issue of whether the rate of erosion can be estimated with enough confidence to predict surface impact from only a short time interval of sounder data. To evaluate this possibility (made more difficult by large-amplitude waves and turbulence), the sounder record height defining the top of the inversion was digitized in progressively longer time sections, calculating a straight-line best fit for each segment. The intersections of these straight lines with the surface show the predicted impact times. These estimates in Fig. 9 show that, after the first half hour, estimates accurate to about ± 1 h were obtained. A similar approach should work equally well for remote sensors of various kinds (e.g., FM/CW radar). This type of prediction

Table 3 Some hazards and practical methods for their detection

System	Technique	Measurement capability	Problem
Thunderstorm outflows and cold fronts	Anemometer arrays[3]	Provides warning of approaching wind shift or pressure-jump lines	Can require high densities for complete coverage
	Pressure-sensor arrays[2]	Same as above	Same as above
	Combined surface systems of pressure and wind sensors[2]	Same as above	Same as above
	Doppler radar[31]	Radial component of windspeed	May not detect outflows of limited depths
Upper-level flow above ground-based inversion	Monostatic acoustic sounder[13]	Small-scale thermal fluctuations	Noise from low-level winds
	FM/CW radar[29]	Radial components of wind speed	Research tool
	Well-positioned surface sensors when obstacle flows are involved[12]	Simple, low-cost method of obtaining remote information from a specific site	Measurements may be nonrepresentative because of local effects
Gravity shear waves at jet stream altitudes	Profiler system[32]	Vertical profiles of wind, temperature, and humidity	Operational version not in production
Downslope windstorms	Doppler radar[31]	Radial component of wind speed	May encounter ground clutter problems near mountains
	Well-positioned surface sensors[12]	Direct measurement of flow changes above lower altitude or distant site	Point measurements may not be representative
Thunderstorm downflows[a]	—	—	—

[a] An extensive experiment in the planning stage (JAWS—Joint Airport Weather Study[33]) will compare possible methods of downflow detection in addition to studying other weather phenomena in an airport environment.

presumes that the erosion rate remains approximately constant. Four events measured during Project AEOLUS showed essentially constant erosion rates.[12]

Such shear events above stable layers have practical importance not only for aircraft operations along the front range (such as small airports close to the foothills), but also for surface pollution and windstorm situations. Similar situations occur involving mountain valleys (frequently the site of small airports serving ski areas).

Detection Methods

Table 3 reviews several wind shear hazards and solutions proposed for their detection, indicating that a variety of techniques can provide useful warnings for segments of the wind shear problem. However, hazards (e.g., thunderstorm downflows) remain with no clear solution in view. It is hoped that close cooperation between those working on numerical simulations of these complex fluid-dynamical processes, simulations of aircraft and pilot response, meteorological prediction, and the application of in situ and remote sensing techniques will eventually provide timely warnings for a broad range of atmospheric wind shear hazards.

Acknowledgments

I am grateful to the personnel of the Field Observing Facility of NCAR for their deployment and operation of the PAM system. Larry Vohs and Lisa Sereno of the Wave Propagation Laboratory of NOAA ensured monostatic acoustic sounder data were available. R. Chadwick and K. Moran operated the FM/CW radar as part of Project AEOLUS. Richard Nagle and Thomas LeFebvre assisted with data reduction for Project AEOLUS.

References

[1] Bromley, E. Jr., "Aeronautical Meteorology: Progress and Challenges—Today and Tomorrow," *Bulletin of the American Meteorological Society,* Vol. 58, Nov. 1977, pp. 1156-1160.

[2] Bedard, A. J. Jr., Merrem, F. H., Simms, D., and Cairns, M. M., "A Thunderstorm Gust-Front Detection System: Part I. System Operation and Significant Case Studies; Part II. Statistical Results," Federal Aviation Administration Rept. FAA-RE-79-55, Aug. 1979.

[3] Goff, R. C., "The Low Level Wind Shear Alert System (LLWSAS)," Federal Aviation Administration Rept. FAA-RD-80-45, FAA-NA-80-1, May 1980.

[4] Fujita, T. T. and Caracena, F., "An Analysis of Three Weather-Related Aircraft Accidents," *Bulletin of the American Meteorological Society,* Vol. 58, Nov. 1977, pp. 1165-1181.

[5] Fujita, T. T., "Manual of Downburst Identification for Project Nimrod," Univ. of Chicago, Chicago, Ill., SMRP Research Paper 156, 1978.

[6] Houbolt, J. C., "Atmospheric Turbulence," *AIAA Journal,* Vol. 11, April 1973, pp. 421-437.

[7] MacCready, P. B. Jr., "Standardization of Gustiness Values from Aircraft," *Journal of Applied Meteorology,* Vol. 3, 1964, pp. 439-449.

[8] Panofsky, H. A. and Press, H., "Meteorological and Aeronautical Aspects of Atmospheric Turbulence," *Progress in Aeronautical Science,* Vol. 3, Macmillan, New York, pp. 179-232.

[9] Goff, R. C., "Vertical Structure of Thunderstorm Outflows," *Monthly Weather Review,* Vol. 104, No. 11, 1976, pp. 1429-1440.

[10] Caracena, F. and Kuhn, P. M., "Remote Sensing of Thunderstorm Outflow Severity with an Airborne IR Sensor," *Conference on Weather Forecasting and Analysis and Aviation Meteorology,* American Meteorological Society, Boston, 1978, pp. 287-292.

[11] Byers, H. R. and Braham, R. R., *The Thunderstorm,* U. S. Dept. of Commerce, Washington, D. C., June 1949.

[12] Bedard, A. J. Jr., Nagle, R., and LeFebvre, T., "Monostatic Acoustic Sounder Measurements During Project AEOLUS 1980: Case Studies Describing the Erosion of Surface-Based Stable Layers," *Proceedings of the International Symposium on Acoustic Remote Sensing of the Atmosphere and Oceans,* Univ. of Calgary, Calgary, Alberta, Canada, 1981.

[13] Hooke, W. H., Young, J. M., and Beran, D. W., "Atmospheric Waves Observed in the Planetary Boundary Layer Using an Acoustic Sounder and a Microbarograph Array," *Boundary-Layer Meteorology,* Vol. 2, 1972, pp. 371-380.

[14] Greene, G. E., Frank, H. W., Bedard, A. J. Jr., Korrell, J. A., Cairns, M. M., and Mandics, P. A., "Wind Shear Characterization," Final Report to the Federal Aviation Administration, Wave Propagation Lab., NOAA, Boulder, Colo., 1977.

[15] Lilly, D. K., "A Severe Downslope Windstorm and Aircraft Turbulence Event Induced by a Mountain Wave," *Journal of Atmospheric Science,* Vol. 35, Jan. 1978, pp. 59-77.

[16] Lilly, D. K. and Lester, P. F., "Waves and Turbulence in the Stratosphere," *Journal of Atmospheric Science,* Vol. 31, April 1974, pp. 800-812.

[17] Förchtgött, J., "Active Turbulent Layer Downwind of Mountain Ridges," *Schweizer Aero-Review,* Bern, Vol. 32, 1957, pp. 324-335.

[18] Olsen, J. H., Goldburg, A., and Rogers, M., eds., *Aircraft Wake Turbulence and Its Detection,* Plenum, New York, 1971.

[19] Crow, S. C., "Stability Theory for a Pair of Trailing Vortices," *AIAA Journal,* Vol. 8, Dec. 1970, pp. 2172-2178.

[20] Vinnichenko, N. K., Pinus, N. Z., Shrmeter, S. M., and Shur, G. N., *Turbulence in the Free Atmosphere,* translated from Russian, edited by J. A. Dutton, Consultants Bureau, N. Y., 1973.

[21] Greene, G. E. and Hooke, W. H., "Scales of Gravity Waves Generated by Instability in Tropospheric Shear Flows," *Journal of Geophysical Research,* Vol. 84, No. C10, 1979, pp. 6362-6364.

[22] Bedard, A. J. Jr., and Sanders, M. J. Jr., "Thunderstorm-Related Wind Shear Detected at Dulles International Airport Using a Doppler Acoustic/Microwave Radar, a Monostatic Sounder and Arrays of Surface Sensors," *Conference on Weather Forecasting and Analysis and Aviation Meteorology,* American Meteorological Society, Boston, 1978, pp. 347-352.

[23] Lee, J. T., Stokes, J., Sasaki, Y., and Baxter, T., "Thunderstorm Gust Fronts—Observations and Modeling," Final Report to the Federal Aviation Administration, FAA Rept. FAA-RD-78-145, Dec. 1978.

[24] Frost, W., Crosby, B., and Camp, D. W., "Flight Through Thunderstorm Outflows," *Journal of Aircraft,* Vol. 16, Nov. 1979, pp. 749-755.

[25] McCarthy, J., Blick, E. F., and Bensch, R. R., "Jet Transport Performance in Thunderstorm Wind Shear Conditions," NASA CR 3207, 1979.

[26] Chadwick, R. B., Moran, K. P., Morrison, G. E., and Campbell, W. C., "Measurements Showing the Feasibility for Radar Detection of Hazardous Wind Shear at Airports," Final Report to the Air Force Geophysics Lab., Wave Propagation Lab., NOAA, Boulder, Colo., 1978.

[27] Brock, F. V. and Govind, P. K., "Portable Automated Mesonet in Operation," *Journal of Applied Meteorology,* Vol. 16, March 1977, pp. 299-310.

[28] Hicks, R. B. and Mathews, T., "Impact on Calgary's Air Quality: Acoustic Sounder Observations of Atmospheric Stability," *Water, Air, and Soil Pollution,* Vol. 11, No. 2, 1979, pp. 159-172.

[29] Chadwick, R. B., Moran, K. P., Strauch, R. G., Morrison, G. E., and Campbell, W. C., "A New Radar for Measuring Winds," *Bulletin of the American Meteorological Society,* Vol. 57, No. 9, 1976, pp. 1120-1125.

[30] Bell, R. C. and Thompson, R. O. R. Y., "Valley Ventilation by Cross Winds," *Journal of Fluid Mechanics,* Vol. 96, Pt. 4, 1980, pp. 757-767.

[31] Kropfli, R. A. and Miller, L. J., "Thunderstorm Flow Patterns in Three Dimensions," *Monthly Weather Review,* Vol. 103, No. 1, 1975, pp. 70-71.

[32] Hogg, D. C., Guiraud, F. O., Little, C. G., Strauch, R. G., Decker, M. T., and Westwater, E. R., "Design of a Ground-Based Remote Sensing System Using Radio Wavelengths to Profile Lower Atmospheric Winds, Temperature, and Humidity," *Remote Sensing of Atmospheres and Oceans,* edited by A. Deepak, Academic Press, New York, 1980, pp. 313-359.

[33] McCarthy, J., Fujita, T. T., and Wilson, J., "Project JAWS," National Center for Atmospheric Research, Boulder, Colo., Informal Planning Document, 1980.